01 Jun 2019

A Phenomenological Model Of Non-Linear Loss In Ferrimagnetic Frequency-Selective Limiters

Anatoliy Boryssenko

Scott Gillette

Marina Koledintseva
Missouri University of Science and Technology, marinak@mst.edu

Recommended Citation

A. Boryssenko et al., "A Phenomenological Model Of Non-Linear Loss In Ferrimagnetic Frequency-Selective Limiters," *IEEE MTT-S International Microwave Symposium Digest*, pp. 595 - 598, article no. 8701071, Institute of Electrical and Electronics Engineers, Jun 2019.
The definitive version is available at https://doi.org/10.1109/mwsym.2019.8701071

A Phenomenological Model of Non-Linear Loss in Ferrimagnetic Frequency-Selective Limiters

Anatoliy Boryssenko[1], Scott Gillette[2], Marina Koledintseva[2]
[1]A&E Partnership, USA
[2]Metamagnetics, USA
anatoliy@ae-partnership.com, sgillette@mtmgx.com, mkoledintseva@mtmgx.com

***Abstract*—Operation of ferrimagnetic frequency-selective limiters (FSL) is based on non-linear absorption in magnetized ferrite films at RF/microwave power levels exceeding some threshold. A new phenomenological model of non-linear loss in a ferrite medium has been proposed, and it has been implemented in an efficient numerical algorithm for an FSL performance prediction.**

***Keywords*—Frequency-selective limiter, ferrimagnetic, spinwave, power threshold, non-linear loss, transmission line, effective mode index, characteristic impedance.**

I. Introduction

Frequency-selective limiters (FSL) prevent blocking, jamming, and overloading in broadband RF/microwave receiver front-ends due to large-amplitude interfering input signals appearing at some frequencies [1], [2]. Such unwanted signals must be suppressed without affecting smaller-amplitude useful signals at the other frequencies, *i.e.*, signals of interest. FSL operation is based on non-linear absorption effect in a ferrimagnetic (ferrite) medium due to excitation of spin-wave instabilities at the RF/microwave power levels exceeding some threshold level [3]-[8]. Low-power signals pass through this device without significant attenuation, while high-power signals are simultaneously damped, thus providing a frequency selective limiting ability. Frequency-selective limiting at frequencies of above-threshold interferences takes place automatically within the instantaneous bandwidth of the FSL, and an FSL in this sense is an automatic self-tuned device, though the center frequency of the instantaneous bandwidth can be tuned by external bias magnetic field [2], [3], [9]-[11]. FSLs demonstrate superior performance as compared to traditional approaches using limiting/clipping diode circuits and adaptive compensation schemes with prior knowledge of interferers [1], [9]-[12].

Ferrite-based FSL design is not straightforward. FSL design requires modeling of non-linear behavior of material parameters (specifically, permeability and magnetic loss) since FSL's operation depends strongly on the RF/microwave power. No existing commercial computational electromagnetics tools support modeling of non-linear magnetic interactions at high frequencies. To implement such non-linearity, a rigorous, or at least adequate approximate preliminary analytical formulation is required.

Most of the reported design approaches for FSL are empirical and combine the available commercial and in-house numerical codes and custom design tools, which are neither fully completed, nor integrated. No systems-level "black-box" models exist for FSL. Therefore, filling in this gap is of high importance in general, and immediately applicable for FSL design. This work is based on the phenomenological model [8], and a number of closed-form expressions are derived to allow for efficient numerical modeling of non-linear loss associated with magnetic spinwave instability. Here, examples of phenomenological model implementation are demonstrated for cases of FSLs on co-planar waveguides (CPW) for X/Ku bands and the model is linked with a commercial Multiphysics numerical modeling tool COMSOL [13].

II. Slice Decomposition Model of FSL

The phenomenological model predicts power loss in nonlinear ferrimagnetic materials versus a number of design parameters such as input power, frequency, external bias magnetic field, and various design parameters - geometrical and material. To build the model, the "traveling power wave" approach [9] is employed. A linear TEM waveguiding structure is sliced along the direction of wave propagation, z [11], as is shown in Fig. 1. Cascading all the individual slices in a circuit model allows for predicting the key FSL features, including power- and frequency-dependent insertion loss. Since each i^{th} slice is a short TEM segment, it can be characterized by the corresponding effective mode index $n_{eff,i}$ and characteristic impedance $Z_{0,i}$, $i=1...N$. These parameters can be found by solving numerically a non-linear eigenmode problem, where the waveguide properties vary depending on the intensity of the internal RF/microwave fields. In this work, non-linear eigenmodes are proposed to find in two steps using, for example, COMSOL RF Module [13]. Fig. 2 shows the meshed cross-sectional views of the CPW with ferrimagnetic films for modeling in COMSOL.

First, the linear "small-signal" eigenmode solution is computed, and the typical E- and H-fields for the eigenmode are illustrated in Fig. 3. Next, for each set of input power, frequency, and magnetic field bias H_0, the non-linear "large-signal" eigenmode solutions are computed in a few iterations. This is done in COMSOL by changing locally electrical properties of the meshed elements that experience different losses depending on their local H-field magnitude. Some details for the algorithm and illustrations are given in Section III. The entire computational process is fully scripted in MATLAB to launch the COMSOL engine, automate parametric sweeps, and collect all the mode data in look-up tables. The mode parameters $n_{eff,i}$ and $Z_{0,i}$ are explained and illustrated in Section IV, and computed FSL power limiting is presented and compared with experiment in Section V.

978-1-7281-1309-8/19/$31.00 © 2019 IEEE

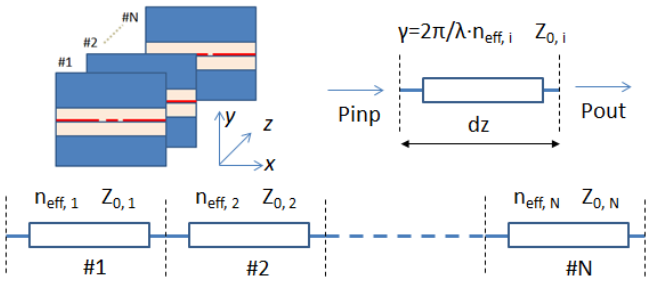

Fig. 1. FSL slice model (left-top) made of short transmission line with effective mode indices $n_{eff\,i}$ and characteristic impedances Z_{0i} (top-right), and the entire model is cascaded of N slices to predict the insertion loss (bottom).

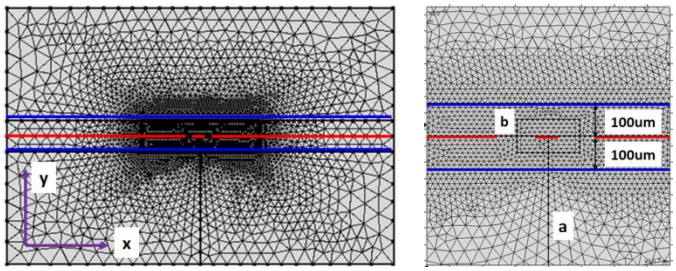

(a) (b)

Fig. 2. Cross-sectional views with the mesh in COMSOL for the 2.5x1.6 mm overall-size CPW with signal traces (in the center, marked in red), 100 μm thick ferrimagnetic films outlined beneath and above CPW (in blue), and voltage "a" and current "b" integration paths: (a) complete cross-sectional geometry; (b) central portion magnified to show the very fine mesh.

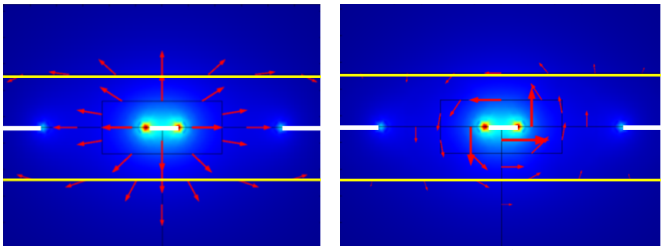

(a) (b)

Fig. 3 . EM field distributions solved in COMSOL for the CPW TEM mode and rendered in a normalized logarithmic scale for the central CPW portion: (a) electrical field; (b) magnetic field.

III. Phenomenological Power Loss Model in FSL

Non-linear absorption occurs in ferrites, when local magnetic field intensity exceeds a certain critical material-specific threshold level [9],[10]. The critical H-field components - parallel, $H_{crit}^{||}$, and perpendicular, $H_{crit}^{\perp}$, as well as mutual orientations between the external magnetic bias field vector and internal RF/microwave magnetic transversal field can be pre-computed for any particular ferrite material [3]. For the case of a monocrystalline yttrium iron garnet (YIG) ferrite with saturation magnetization of $4\pi M_s = 1780\ G$, the dependencies of critical RF magnetic field components versus input frequency and the external magnetic bias H_0 are plotted in Fig. 4.

The RF H-field distribution of non-linear "large-signal" eigenmode (Fig. 3b) must be re-normalized for every given value of the input power. The ordinary linear "small-signal" eigenmode is solved without forcing right-hand side terms and, thus, is power invariant. An iterative procedure is introduced to re-normalize "large-signal" modes to a prescribed level of input power at the CPW cross-section has been proposed and implemented in COMSOL. It is based on the fact that not absolute values but relative values of the H-field with respect to H_{crit} are needed. Thus, a power scaling factor can be introduced and then iteratively adjusted as illustrated by Fig. 5 when the "set" eigenmode power is gradually converged to the actual "computed" eigenmode power. When re-normalization is done, then the H_x and H_y components can be compared with the critical $H_{crit}^{||}$ and $H_{crit}^{\perp}$ values, respectively, and the electrical properties for each mesh element in the CPW cross-section (Fig. 2) can be adjusted according to the phenomenological loss theory outlined below.

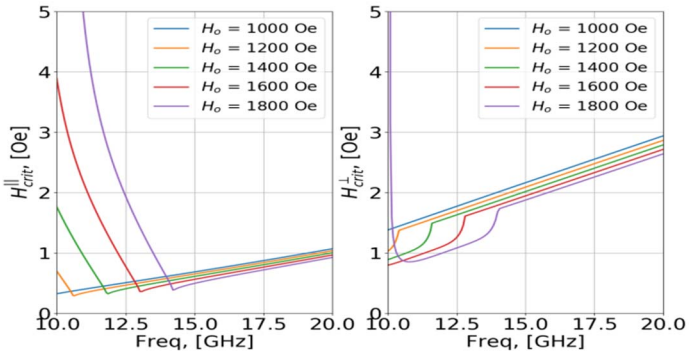

Fig.4. Critical magnetic field vs. frequency for various static bias H-field for parallel (left) and perpendicular (right) pumping RF magnetic field.

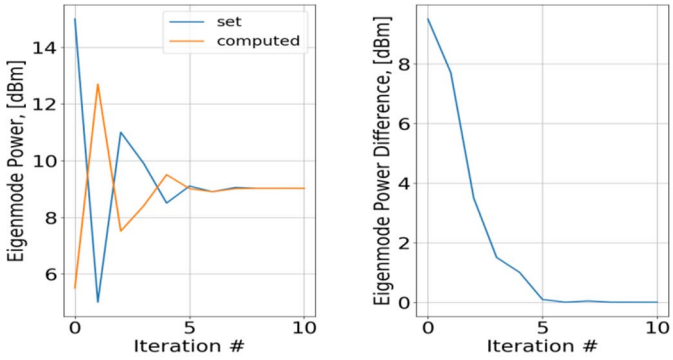

Fig.5. Typical convergence of the nonlinear eigenmode solutions: (left) prescribed and computed power; (right) difference of two.

In particular, the amount of local non-linear (NL) absorbed power in a small volume dV with the local RF magnetic field intensity H at the angular frequency ω is

$$P_{abs}^{NL} = \mu\omega D(\omega) H_{crit}^2 dVF\left(\frac{H}{H_{crit}}\right). \qquad (1)$$

In (1), $D(\omega)$ is the dispersion function defined for parallel || and perpendicular ⊥ RF pumping conditions as follows:

$$D^{||}(\omega) = \frac{\omega_m}{\sqrt{\omega^2+\omega_m^2}-\omega_m}, \qquad (2)$$

$$D^{\perp}(\omega) = \frac{\omega_m}{\omega-\omega_0}, \qquad (3)$$

and the threshold function vs. $x = H/H_{crit}$ is

$$F(x) = \begin{cases} 0, & x < 1 \\ \sqrt{x^2 - 1}, & x \geq 1 \end{cases}, \quad (4)$$

where $\omega_0 = \mu_0 \gamma H_0$ is frequency of spin magnetic moment precession in the internal static magnetic bias field H_0, $\omega_m = \mu_0 \gamma M_s$ is the angular frequency associated with saturation for the magnetization M_s, γ =1.76×10^{11} C/kg is the gyromagnetic ratio. The equivalent power loss can be included in the numerical model of the FSL by considering equivalent magnetic loss tangent $tan\delta_m$, which defines the complex permeability $\dot{\mu} = \mu_0 \mu_r (1 - j tan\delta_m)$. Therefore, the equivalent linear (L) power loss can be described for the small volume dV after some algebraic transformations as follows:

$$P_{abs}^{L} = 0.5 \mu \omega H^2 dV tan\delta_m \quad (5)$$

Equating (1) and (5) yields the final expression for equivalent magnetic loss tangent

$$tan\delta_m^{||(\perp)} = 2D^{||(\perp)}(\omega) G(x) \quad (6)$$

where G is the function of the same argument $x = H/H_{crit}$,

$$G(x) = \frac{F(x)}{x^2} = \begin{cases} 0, & x < 1 \\ \frac{\sqrt{x^2 - 1}}{x^2}, & x \geq 1 \end{cases} \quad (7)$$

Thus, (6) allows for defining the modified local material properties, which depend on the local H/H_{crit} ratios for each mesh element as in Fig. 2. The behavior of the function G(x) is shown in Fig. 6.

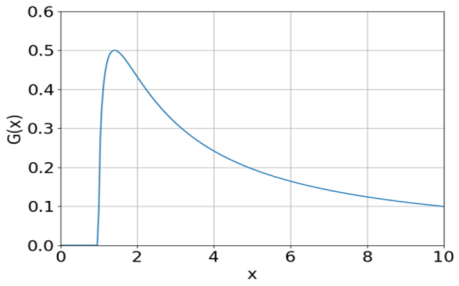

Fig. 6. Dimensionless function (8) which indicates optimum intensity of power absorption rate

Such computations over the meshes can be done in COMSOL. The equivalent magnetic loss tangent can be computed separately for both parallel and perpendicular RF pumping conditions versus the transversal coordinates (Fig. 7). Similarly, the magnetic permeability tensor can be introduced in the COMSOL model,

$$\hat{\mu} = \begin{bmatrix} 1 - j tan\delta_m^{||} & 0 & 0 \\ 0 & 1 - j tan\delta_m^{\perp} & 0 \\ 0 & 0 & 1 \end{bmatrix}. \quad (8)$$

IV. Nonlinear Dispersion Features

Note that maximum absorption due to non-linearity in Fig. 7 are spatially localized in the areas of the ferrite film, where the function (7) plotted in Fig. 6 is maximum, *i.e.*, at $x_0 = \sqrt{2}$, *viz.* $H = \sqrt{2} H_{crit}$. This shows that the maximum absorption is achievable at some optimal level of magnetic field intensity, or input power. If those optimal levels are exceeded, power absorption decreases. This formally occurs when $H > \sqrt{2} H_{crit}$. Implementing the abovementioned model approach in COMSOL allows for computing the key features of the waveguide slices required to build the model as in Fig. 1: the effective mode index n_{eff} (Fig. 8) and characteristic impedance Z_0 (Fig. 9) versus input power and a number of input frequencies.

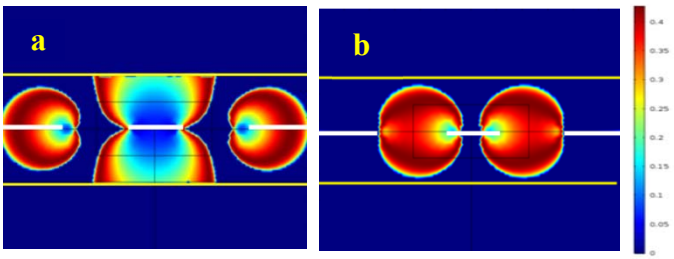

Fig. 7. Magnetic loss tangent for 50 mW input power at 15 GHz computed for: (a) parallel and (b) perpendicular pumping conditions.

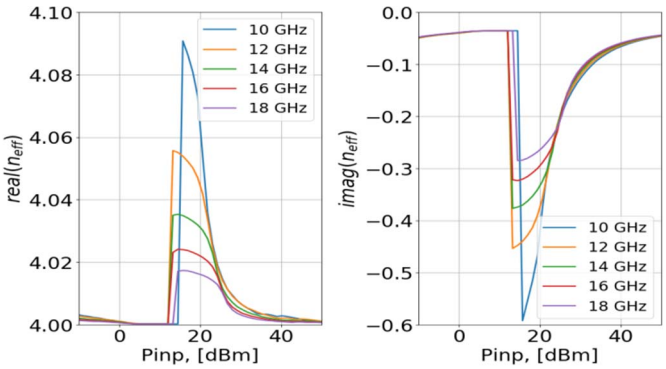

Fig. 8. Complex effective eigenmode index versus input power at several frequencies for $H_0 = 1200\ Oe$: (left) real part; (right) imaginary part.

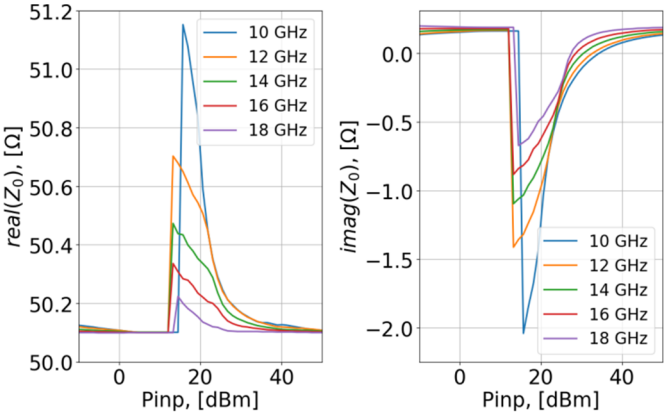

Fig. 9. Complex characteristic impedance versus input power at several frequencies for $H_0 = 1200\ Oe$: (left) real part; (right) imaginary part.

As is shown in Figs. 8 and 9, the approximate threshold power levels are ~12-15 dBm for this particular CPW design (Fig. 2) and the material selection. For the input power above the threshold, the loss is associated with the notable growth of the imaginary parts of the n_{eff} and Z_0 parameters.

V. FSL Performance Prediction

Using the slice features (Figs. 8 and 9) in the model as is shown in Fig. 1, allows predicting the behavior of the FSL with the cross-sectional design shown in Fig. 2. For example, for the 40 mm long device with external H-field bias H_0=1200 Oe, the power versus the device length was computed using 2000 slices, and they are plotted in Fig. 10 for three levels of input power above the 12-15 dBm threshold. The data in Fig. 10 shows, *e.g.*, how power dissipates inside the FSL. Figs. 10 and 11 show the power limiting characteristics; the computed data is in Fig. 11 (a), and validation by measurement is also shown in Fig. 11 (b).

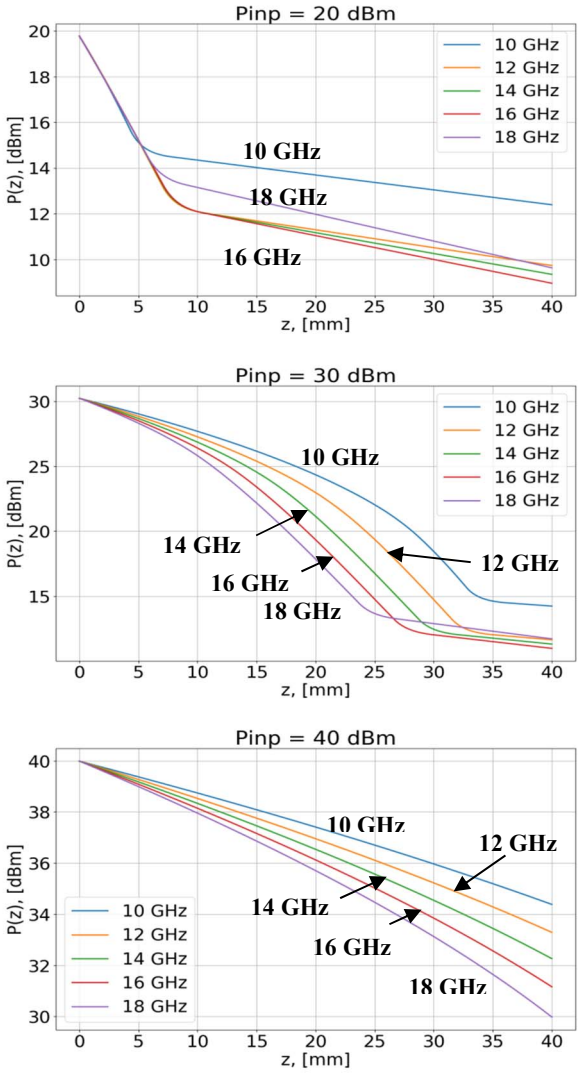

Fig. 10. Output power along the wave propagation z coordinate for a number of input frequencies, bias field 1050 Oe, and at different input power levels.

VI. Conclusion

A set of compact closed-form expressions has been derived and used to build an efficient computer model that allows for predicting non-linear loss in a ferrimagnetic film of a CPW-based FSL design (Fig. 2). Using this computer model frequency-selective power limiting features can be predicted. The proposed phenomenological model provides the design hints based on the deeper understanding of non-linear power loss in ferrimagnetic material, in general, and could be used for the design of FSL devices, in particular.

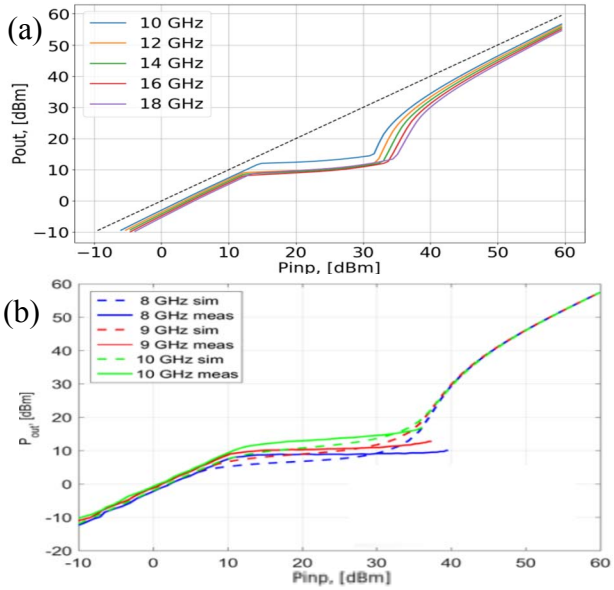

Fig. 11 Output vs. input power for a number of input frequencies, bias field 1270 Oe: (a) modeled results (straight dashed line – no limiting, no loss); (b) modeled (dashed lines) and measured (solid lines).

Acknowledgment

The authors gratefully acknowledge support of this work in part by the Defense Advanced Research Projects Agency (DARPA) under Contract No. W911NF-18-C-0032.

References

[1] R.W. Orth, "Frequency-selective limiters and their application", *IEEE Trans. Electromag. Compat.*, vol. 10, no. 2, pp. 273-283.

[2] J.D. Adam, "Mitigate the interference: Nonlinear frequency selective ferrite devices," *IEEE Microw. Mag.*, vol. 15, no. 6, pp. 45-56, Sep. 2014.

[3] J.D. Adam and F. Winter, "Magnetostatic wave frequency selective limiters", *IEEE Trans. Mag.*, vol. 49, no. 3, Mar. 2013, pp. 956-962.

[4] M. Chen and C.E. Patton, "Spin wave instability in ferrites", in *Nonlinear Phenomena and Chaos in Magnetic Materials*, 1994.

[5] H. Suhl, "The theory of ferromagnetic resonance at high signal powers", *J. Phys. Chem. Solids*, vol. 1, no. 4, Jan. 1957, pp. 209-227.

[6] E. Schlömann and R.I. Joseph, "Instability of spin waves and magnetostatic modes in a microwave magnetic field applied parallel to the dc field", *J. Appl. Phys.*, vol. 32, no. 6, Jun. 1961, pp. 1006-1014.

[7] F.R. Morgenthaler, "Survey of ferromagnetic resonance in small ferrimagnetic ellipsoids", *J. Appl. Phys.*, vol. 31, no. 5, 1960, pp. 95S-97S.

[8] M. Chen and C.E. Patton, "Spin wave instability processes in ferrites" in *Nonlinear Phenomena and Chaos in Magnetic Materials,* ed. P.E. Wigen, 1994, World Scientific Publishing, Singapore, pp. 33-82.

[9] S.N. Stitzer and H. Goldie, "A multi-octave frequency selective limiter," *IEEE MTT-S International Microwave Symposium Digest*, Boston, MA, USA, 1983, pp. 326-328.

[10] J.D. Adam and S.N. Stitzer, "Frequency selective limiters for high dynamic range microwave receivers," *IEEE Trans. on Microwave Theory and Techniques*, vol. 41, no. 12, pp. 2227-2231, Dec. 1993.

[11] S.M. Gillette, M. Geiler, J.D. Adam, A. L. Geiler, "Ferrite-based reflective-type frequency selective limiters", *IMWS-AMP on Advanced Materials and Processes for RF and THz Applications*, 2018.

[12] A.J. Giarola, "A review of the theory, characteristics, and operation of frequency selective limiters", *IEEE Proceedings*, vol. 67, Oct. 1979, p. 1380-1396.

[13] COMSOL RF Module, https://www.comsol.com/rf-module